

4 Ionosphere and Thermosphere

4-1 Derivation of TEC and Estimation of Instrumental Biases from GEONET in Japan

MA Guanyi and MARUYAMA Takashi

This paper presents a method to derive the ionospheric total electron content (*TEC*) and to estimate the biases of GPS satellites and dual frequency receivers using the GPS earth observation network (GEONET) in Japan. Based on the consideration that the *TEC* is uniform in a small area, the method divides the ionosphere over Japan into 32 meshes. The size of each mesh is 2° by 2° in latitude and longitude, respectively. By assuming that the *TEC* is identical at any point within a given mesh and the biases do not vary within a day, the method arranges unknown *TECs* and biases with dual GPS data from about 209 receivers in a day unit into a set of equations. Then the *TECs* and the biases of satellites and receivers were determined by using the least squares fitting technique. The performance of the method is examined by applying it to geomagnetically quiet days in various seasons, and then comparing the GPS-derived *TEC* with ionospheric critical frequencies (f_oF_2). It is found that the biases of GPS satellites and most receivers are very stable. The diurnal and seasonal variation in *TEC* and f_oF_2 shows a high degree of conformity. The method using highly dense receiver network like GEONET is not always applicable in other areas. Thus the paper also proposes a simpler and faster method to estimate a single receiver's bias by using the satellite biases determined from GEONET. The accuracy of the simple method is examined by comparing the receiver biases determined by the two methods. Larger deviation from GEONET derived bias tends to be found in the receivers at lower (<30°N) latitudes due to the effects of equatorial anomaly.

Keywords

Mid-latitude ionosphere, Instruments and techniques, Radio wave propagation

1 Introduction

The total electron content (*TEC*) is one of the most important parameters used in the study of the ionospheric properties. Acting as a dispersive medium to Global Positioning System (GPS) satellite signals, the ionosphere causes a group delay and a phase advance to the radio waves propagate from a GPS satellite to a ground-based receiver. *TEC* can be obtained from the difference in the group

delays of dual-frequency GPS observations. However, there exists an instrumental delay bias in each signal of the two GPS frequencies. Their difference, referred to as instrumental or differential instrumental bias, affects the accuracy of the *TEC* estimation greatly. The combined satellite and receiver biases can even lead to a negative *TEC*.

The task of assessing GPS satellite and receiver biases has been assumption dependent and time consuming. Assuming that 1) the

electron distribution lies in a thin shell at a fixed height above the Earth; 2) the *TEC* is time-dependant in a reference frame fixed with respect to the Earth-Sun axis; 3) the satellite and receiver biases are constant over several hours, several authors (Lanyi and Roth, 1988; Coco et al., 1991) made their analysis with data from a single station during local nighttime, and they modeled the vertical *TEC* by a quadratic function of latitude and longitude. Wilson et al. (1992; 1995) extended the thin spherical shell fitting technique to data sets from a GPS network in a 1-day or 12-h unit, and represented the vertical *TEC* as a spherical (surface) harmonic expansion in latitude and longitude. Sardón et al. (1994) modeled the vertical *TEC* as a second-order polynomial in a geocentric reference system, where the coefficients of the polynomial are simulated with random walk stochastic processes. The coefficients (and hence, the *TEC*) and instrumental biases are then estimated by using a Kalman filtering approach. A common feature of the previous works is that an assumption of a rather smooth ionospheric behavior had to be introduced in the studies. Recently, with data collected from more than 1000 receivers of the GPS earth observation network (GEONET) in Japan, Otsuka et al. (2002) produced two-dimensional maps of the *TEC* having high spatial resolution of 0.15° by 0.15° in latitude and longitude. Although they removed the instrumental biases in order to derive the absolute vertical *TEC*, they did not discriminate the satellite and receiver biases separately.

In this paper, we present a method to derive the *TEC* over Japan, and estimate the biases of GPS satellites and the dual P-code receivers that are part of GEONET in Japan. Our method is different from that of Otsuka et al. (2002) in that along with the *TEC*, both the satellite and the receiver biases can be obtained. The algorithm is depicted in detail in **2**. We show in **3** the results of an application of the proposed method to three geomagnetically quiet days in the summer, autumn and winter of 2001, respectively. After the

stability of the satellite biases is shown, day-to-day variation in instrumental bias are discussed. Evaluation of the GPS-derived *TEC* is made by comparison with ionosonde's ionospheric critical frequency (referred to as f_oF_2) observations. Discussion on the accuracy of the GEONET based method is presented with the goodness of fit to the data. We propose in **4** a simpler and faster method to estimate a single receiver's bias by using its GPS observations and known satellite biases. The accuracy of the method is manifested by applying it also to the 9 days and by comparing the results with those in **3**. The main results obtained are summarized in **5**. Finally, the conclusions drawn are presented in **6**.

2 Algorithm

2.1 *TEC* extraction from GPS observation

There are 28 GPS satellites currently orbiting the Earth at an inclination of 55° and at a height of 20,200 km. They broadcast information on two frequency carrier signals, which are 1.57542 GHz (referred to as f_1) and 1.2276 GHz (referred to as f_2), respectively. GPS observations give two distances (known as pseudorange) and two phase measurements corresponding to the two signals. Because of the dispersive nature of the ionosphere, the two radio signals are delayed by different amounts (known as group delay) and their phases are advanced when they propagate from a satellite to a receiver on the Earth. The slant path TEC_{sl} from a satellite to a receiver can be obtained from the difference between the pseudoranges (P_1 and P_2), and the difference between the phases (L_1 and L_2) of the two signals [Blewitt, 1990]

$$TEC_{slp} = \frac{2(f_1 f_2)^2}{k(f_1^2 - f_2^2)} (P_2 - P_1) \quad (1)$$

$$TEC_{sl} = \frac{2(f_1 f_2)^2}{k(f_1^2 - f_2^2)} (L_1 \lambda_1 - L_2 \lambda_2) \quad (2)$$

where k , related to the ionosphere refraction, is $80.62 \text{ (m}^3/\text{s}^2)$. λ_1 and λ_2 are the wavelengths corresponding to f_1 and f_2 , respectively.

Because of the 2π ambiguity in the phase measurement, TEC_{sl} from the differential phase is a relative value, but it has higher precision than TEC_{slp} . To retain phase path accuracy for the slant path TEC_{sl} , TEC_{sl} are fitted to TEC_{slp} , introducing a baseline, B_{rs} , for the differential phase related TEC_{sl} [Mannucci, et al., 1998; Horvath and Essex, 2000].

$$TEC_{sl} = TEC_{slp} + B_{rs} \quad (3)$$

If having N measurements, the baseline B_{rs} in this paper is computed as the average difference between pseudorange derived TEC_{slp_i} and phase derived TEC_{sl_i} over the index i from $i = 1$ to $i = N$ inclusive.

$$B_{rs} = \frac{\sum_{i=1}^N (TEC_{slp_i} - TEC_{sl_i}) \sin^2 \alpha_i}{\sum_{i=1}^N \sin^2 \alpha_i} \quad (4)$$

where the square sine of satellite's elevation α_i are included as weighting factor, as the pseudorange with low elevation angle is apt to be affected by the multipath effect and the reliability decreases. Consequently the contribution to the baseline determination is greatly depleted from slant paths with low elevations. When making the above calculation of B_{rs} , a data-processing step is included to identify possible cycle-slips in either L_1 or L_2 phase measurements [Blewitt, 1990]. Thus, this study works with pseudorange-leveled carrier phases that are free of ambiguities and have lower noise and multipath effects than the pseudoranges. With 30-second time series of dual GPS data, this part of the process is done for each pair of satellite-receiver independently. The obtained slant path TEC_{sl} then gets rid of all effects on the phases and pseudoranges that are common to both frequencies (such as distance of receiver-satellite, clock offsets, tropospheric delay, etc.), but frequency-dependent effects, like multipath and the differential instrumental biases in the satellite and the receiver, are still present.

To convert to a vertical TEC from a slant path TEC_{sl} , the ionosphere is assumed to be a

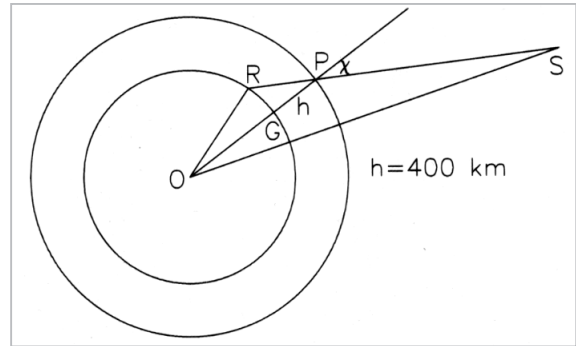


Fig. 1 Geometry of a GPS satellite (S), the ionosphere, and a receiver (R).

While the total electron content is retained, the ionosphere is assumed to be a screen sphere lying at the height of 400 km from the ground. Here P represents intersection of line of sight and the ionosphere, χ is zenith angle.

thin screen shell encircling the Earth and its center to be the same as that of the Earth. The geometry of the GPS satellite, receiver and the ionosphere is shown in Fig.1. The intersection of the slant path from the satellite (S) to the receiver (R) through the ionosphere is referred to as piercing point (P). The zenith angle χ is expressed as the following,

$$\chi = \arcsin\left(\frac{R_e \cos \alpha}{R_e + h}\right) \quad (5)$$

where α is the elevation angle of the satellite, R_e is the mean radius of the Earth, and h is the height of the ionospheric layer, which is assumed to be 400 km in this paper. Further, setting satellite and receiver biases as b_s and b_r , respectively, then the vertical TEC is,

$$TEC = (TEC_{sl} - b_s - b_r) \cos \chi \quad (6)$$

The determination of the absolute TEC and the instrumental biases will be described following an introduction of GEONET, a dense GPS receiver network in Japan.

2.2 GEONET in Japan and mesh division

GEONET is a GPS Earth Observation Network set up by Geographical Survey Institute (GSI) of Japan. It has more than 1000 GPS receivers spread over Japan [Miyazaki et al., 1997], about 209 of which give precise

the receiver number. Because it is not possible to determine unambiguously all the satellites and receiver biases absolutely, one of them (normally one receiver) is set to be 0, as a reference. Then with least squares fitting technique, the solution to the above set of equations can be obtained by the singular value decomposition (SVD), which avoids unrealistic solutions of the equation system [Press et al., 1992]. In our practical calculation, the number of equations is about 35,000. It takes about 8 hours to carry out the whole process from reading the GPS data to solving the equation (8) by a personal computer (PC) using Pentium 4 processor.

3 Results of an application of the method

In order to demonstrate the performance of the technique, several days around solstices and equinox of June 15-17, September 20-22, and December 21-23, 2001 were selected, before and during which it is geomagnetically quiet ($K_p < 4$) times. With the procedure described above, instrumental biases and vertical absolute *TEC* over Japan for each day are obtained. The selected reference receiver is located at 34.16°N, 135.22°E, which has more than 10 receivers surrounding it in the same mesh.

3.1 Instrumental biases

Fig.3 shows the estimated satellite biases for the 9 days over a six-month time span, as a function of the day of year. The vertical dashed lines divide the inconsecutive days. Here the biases are those relative to their means that are indicated in the lower part of the panel. For all the satellites each day, the mean of their biases are first computed, this mean is then subtracted from each individual satellite bias [Coco et al., 1991]. Consequently, the systematic trends, such as changes in the reference receiver bias, have been removed from the satellite. Although the mean of satellites biases decreased several ns ($1\text{ns}=2.853\text{TECU}$, $1\text{TECU}=2.853 \times 10^{16} e/m^2$)

from the summer to the winter, the relative biases are quite stable. Among satellite bias difference between inconsecutive days, even the largest value was about 1 ns. The standard deviation in bias was from 0.076 ns to 0.664 ns for the satellite biases for the 9 days. It is less than 0.5 ns for 19 of the 28 satellites. So, the day-to-day variation was very small for satellite biases.

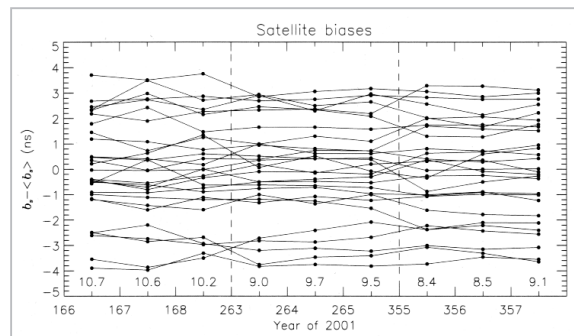


Fig.3 GEONET derived satellite biases for 9 days over a six-month time span, where shown is relative bias referring to the bias with the mean of the day removed. The mean of the satellite biases are shown in the lower part of the panel. Vertical dashed lines divide inconsecutive days.

The day-to-day variation of the estimated receiver biases was also small for most of the receivers. The distribution of the standard deviation of the receiver biases to the 9-day mean is shown in Fig.4. The greatest value was about 4 ns. There were 69% receivers whose standard deviation in bias was smaller than 1 ns; 93% less than 2 ns. Shown in Fig.5, a scatter diagram relates the standard deviation in receiver bias for the 9 days to geographical position of the receiver. It is evident that there is no latitude dependence of the receiver bias variation. This implies that ionospheric local characteristics have little effects on the instrumental bias determination. In spite of this, it is noticeable in Fig.4 that there are several receivers (in mid-latitudes) with large day-to-day variation of biases. There might be several reasons for this, for example: (1) the unstableness in the receiver circuit itself; (2) bias variation of the reference receiver; (3) multipath effects. It is likely that the unstableness in the receiver is the most

reasonable reason, because the bias variation of the reference receiver would affect all the other receivers, and the multipath effects would not vary greatly day by day.

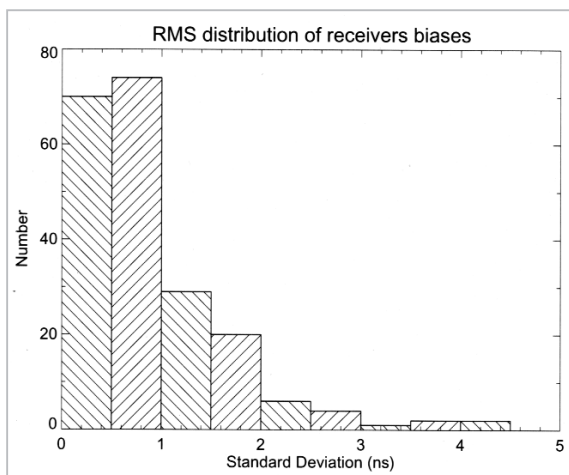


Fig.4 Distribution of the standard deviation of the GEONET derived receiver biases from the 9-day mean. 93% of the cases are within 2 ns.

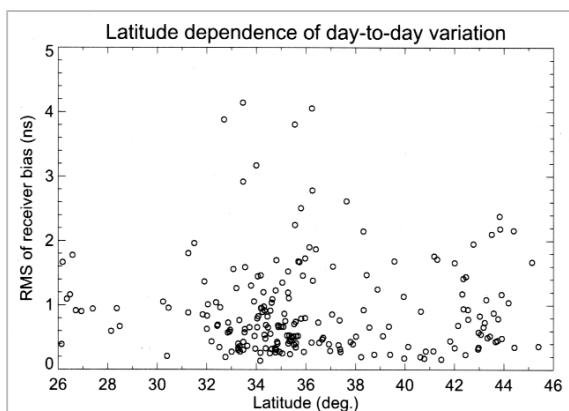


Fig.5 Latitude variation of the standard deviation of the GEONET derived receiver biases from the 9-day mean. No systematic trend can be found.

3.2 GPS-derived TEC

With the method described in 2, *TEC* over Japan can be determined at the same time as the instrumental biases. 15-min time series of *TEC* is shown in the top panel of Fig.6 for the 9 days from the summer to winter of 2001 for a mesh at (35°N, 139°E). The vertical dashed lines separate inconsecutive days. In addition to diurnal features, seasonal variation is conspicuous. Data obtained by other observation techniques are useful for a verification of the

GPS-derived *TEC*. Bottom-side sounding by ionosonde is operated routinely every 15 min at Kokubunji (35.7°N, 139.5°E). The value foF_2 , shown in the middle panel in Fig.6, is used to evaluate the accuracy of the GPS-derived *TEC*. As is evident, the behavior of *TEC* is strikingly similar to that of the foF_2 . The variation in *TEC* and foF_2 shows a high degree of conformity. This is also obvious for fine structures that display in daytime. These facts indicate that the GPS-derived *TEC* is mainly contributed from electrons in F2 region. A more detailed comparison, the ratio of *TEC* to the square of foF_2 is presented in the bottom panel for the 9 days in Fig.6. The diurnal and seasonal variation is clearly displayed. While the daytime level of the ratio is not much different from the summer to the autumn, it doubles in the winter, suggesting greater contribution from the plasmaspheric electron content.

Fig.7 shows contour maps of *TEC* over Japan in the summer, the autumn and the winter in 2001. The *TEC* distribution has a simple pattern in the summer. The daytime *TEC* in the autumn has both a larger value and a

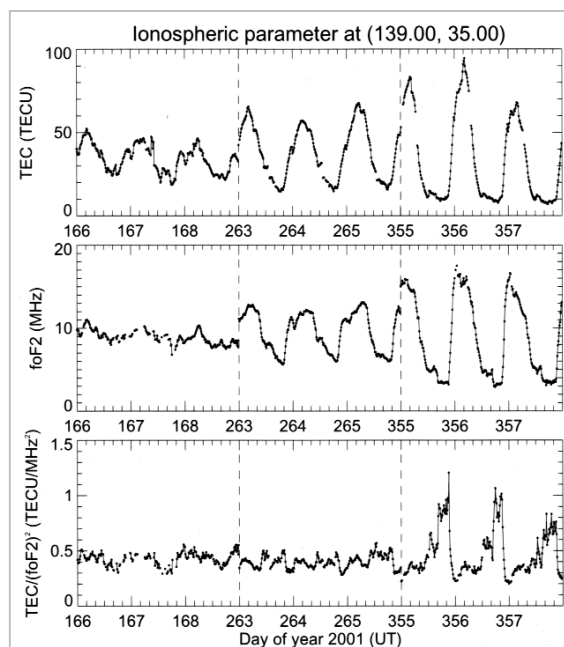


Fig.6 15-min time series of *TEC* at 35°N, 139°E for 9 days over a six-month time span. Vertical lines divide inconsecutive days. Also shown are 15-min time series of foF_2 , the ratio of *TEC* to the square of foF_2 .

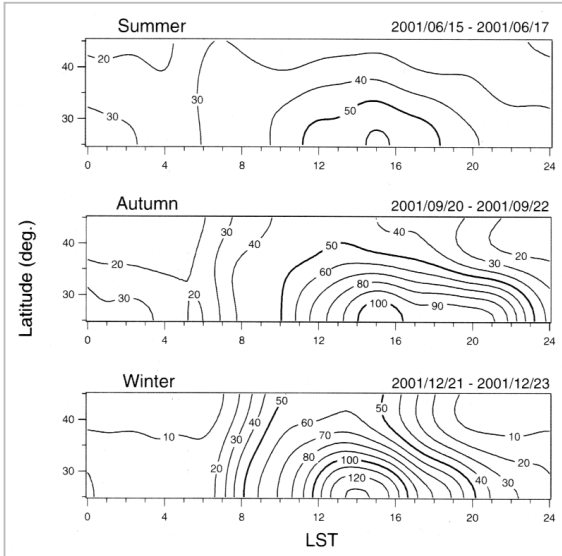


Fig.7 Ionospheric TEC distribution over Japan in the summer, the autumn, and the winter of 2001.

Contours are labeled in units of TECU and the spacing is 10 TECU.

larger gradient in latitude than that in the summer. It is further larger in the winter than that in the autumn. Nighttime TEC value in the winter is about half of that in the other two seasons.

3.3 Accuracy evaluation of the method

The standard deviation of the data from the fitting parameters (residuals) is used to measure how well the estimated parameters agree with the data [Bevington, 1969].

$$\chi_g = \sqrt{\frac{\sum_{i=1}^L (TEC_{sljk} - \sec \chi_{jk} TEC_i - b_{sj} - b_{rk})^2}{L-4}} \quad (9)$$

where L is the number of the slant path TEC_{sl} data (refer to section 2.3). Table 1 lists the χ_g values for the 9 days analyzed. χ_g is less than 5 TECU for 7 days. It is about 8 TECU on Jun. 16, 2001 (167). χ_g is about 51 TECU on Sep. 22, 2001 (265). Individual residual

Table 1 The standard deviation of residual (χ_g) from the GEONET based method for the 9 days in 2001. The numbers in the first row refers to the day of year 2001. The unit of χ_g is in TECU.

DOY	166	167	168	263	264	265	355	356	357
χ_g	3.99	7.94	4.24	3.59	2.81	51.43	3.05	2.76	2.57

for each data point is examined for the day 265, on which χ_g is extremely large. On the day the number of slant path TEC_{sl} data used is 47,400. There are 12,991 data satisfying that $|TEC_{sljk} - \sec \chi_{jk} TEC_i - b_{sj} - b_{rk}| < 1$; there are 23,695 data that $|TEC_{sljk} - \sec \chi_{jk} TEC_i - b_{sj} - b_{rk}| < 2$. There are 40,539 data satisfying $|TEC_{sljk} - \sec \chi_{jk} TEC_i - b_{sj} - b_{rk}| < 5$. That is to say the fitting results agree well with most of the data. Further it is found that most of the large residuals are from those meshes at latitudes lower than 35° ; among 1233 data yielding $|TEC_{sljk} - \sec \chi_{jk} TEC_i - b_{sj} - b_{rk}| > 10$, 950 data are from meshes at latitudes lower than 35° . It is probable that steep latitude gradient in the low latitude ionosphere, created by the development of equatorial anomaly in equinox, caused the large standard deviation in the fitting on the day 265. Thus the large residuals mainly come from the TEC gradient within meshes at lower latitudes. A large χ_g , however, does not necessarily mean the low fitting accuracy of the instrumental biases; the estimated satellite biases on the day 265 do not differ very much from those on the day 264 as seen in Fig.3. A

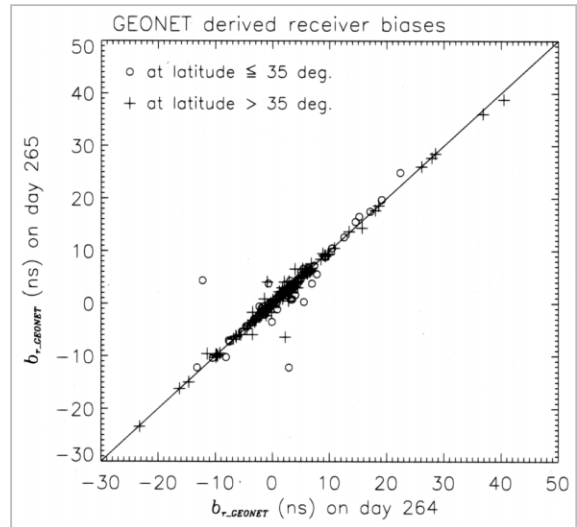


Fig.8 Comparison of GEONET derived receiver biases on the day 265 with those on the 264.

As shown in the figure, the circles represent those receivers located at latitude 35° or lower than 35° , and the crosses refer to the receivers at higher latitudes. No matter where the receivers are, both circles and crosses gather along the diagonal, showing nice agreement between receiver biases estimated on the two different days.

comparison of the receiver biases on the two days is shown with a scatter plot in Fig.8. The circles in the figure represent those receivers located at latitudes $\leq 35^\circ$, and the crosses refer to the receivers at latitudes $> 35^\circ$. The agreement between the biases for the two days is very well regardless the receiver latitude, although moderate deviation can be found for a few receivers. Thus, even for the worst case in terms of residual, the method determines the instrumental biases with a high accuracy.

4 Estimation of bias for a single receiver

The method described in the above section is not always applicable to any situation because the technique is based on a highly dense receiver network in a small area. Also the algorithm requires lengthy processing time, which does not meet the requirement of monitoring the ionosphere in nearly real-time. However, once the satellite biases are determined by using GEONET, those values can be commonly used in any other locations in the globe, where even single receiver is installed. This section will describe a simple and fast method to estimate the bias of a single receiver using the satellite biases determined by GEONET, and evaluate the accuracy of the simple method.

4.1 A simple method

Generally, one GPS receiver simultaneously receives signals from 5 or more GPS satellites at any time. The elevation angle of those satellites could vary widely. The piercing points would be scattered widely but within a limited area, roughly 23° in longitude and 32° in latitude, with the receiver at the center. From different satellites with different elevations the lines of sight to the receiver lead to a spatial variation of slant path TEC_{sl} at any observation time. If the ionosphere is horizontally homogeneous and instrumental biases are correctly removed, the vertically converted $TECs$ should be identical for all of the satellite. In an actual case, in which the ionosphere

has a horizontal gradient and vertical structure, the scattering of vertical $TECs$ is assumed to be the smallest when the instrumental biases are correctly removed. As the satellite biases are well determined by GEONET and shown to be stable (refer to **3**), which are used as known values hereafter, the receiver bias is estimated independently from GEONET by trying a series of bias candidates and finding out the one that gives a minimum deviation of $TECs$ to their mean. In mathematical description, given a trial receiver bias $b(i)$, the standard deviation of $TECs$ to their mean is calculated at each observation time. Then the total standard deviations, $\Sigma\sigma_i$, is obtained for the whole day. The value of the $b(i_0)$ when $\Sigma\sigma_i$ takes the minimum value, $\Sigma\sigma$, is considered to be a correct receiver bias (hereafter, referred to as fitted receiver bias). It takes only several minutes to get the fitted receiver bias by a personal computer (PC) using Pentium 4 processor.

When different receiver biases are applied, the dispersion of vertical $TECs$ is examined by using actual data set. For the convenience of comparison, one receiver is chosen from GEONET, which is located at 35.53°N , 137.89°E . The results for the observations on June 17, 2001 are given in Fig.9. The dashed lines are for slant path TEC_{sl} from the satellites to the receiver. The solid lines represent vertically converted $TECs$ after the satellite and receiver biases are removed. For the three panels, the satellite biases were identical and determined with the method described in **3**, but the receiver bias was taken to be different: in the top panel, the receiver bias is GEONET-derived one; in the lower two panels, the receiver biases were arbitrarily chosen so that it is much less than the GEONET-derived one in the middle panel, and much larger than the GEONET-derived one in the bottom panel. The corresponding value of $\Sigma\sigma_i$ for each case is shown at the top right corner. It is evident that when inappropriate receiver bias is applied, the curves do not converge.

Fig.10 shows variation of $\Sigma\sigma_i$ as a function of $b(i)$ for the same data set. From the

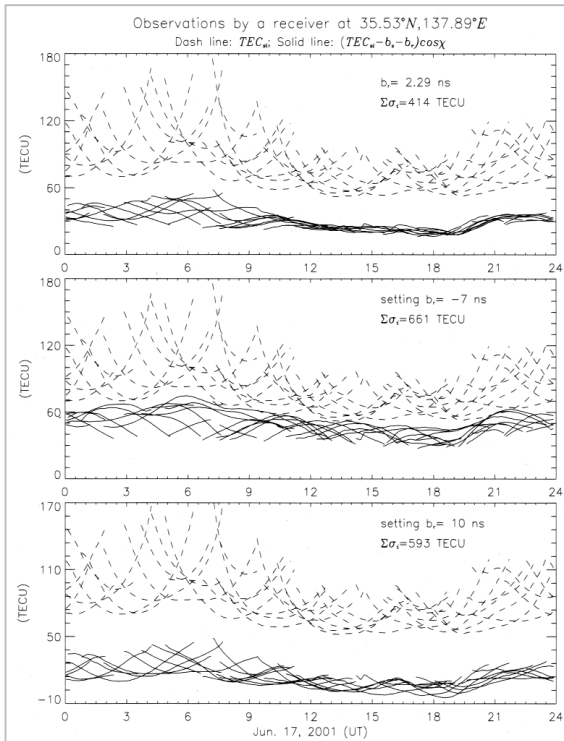


Fig. 9 Slant path TEC_{sl} (dash lines) from GPS satellites to a receiver at $35.53^\circ N$, $137.89^\circ E$.

The solid lines are vertical TEC converted from TEC_{sl} with the instrumental biases removed. The satellite biases are GEONET derived. The receiver bias is GEONET derived in the top panel. They are assumed values in the lower two panels. The one day sum of standard deviation of $TECs$ to their mean at any time, $\Sigma\sigma_p$, is shown in each panel.

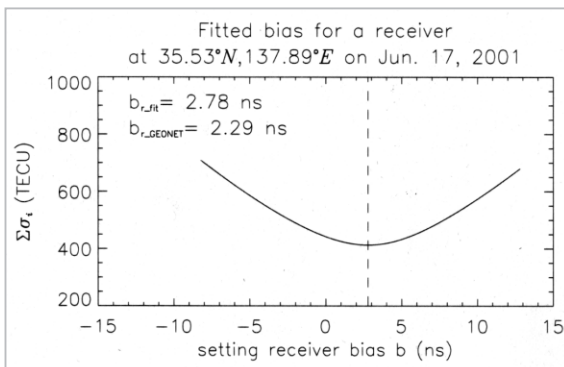


Fig. 10 Fitted bias to a receiver at $35.53^\circ N$, $137.89^\circ E$.

The GEONET derived bias value, 2.29 ns, is also given.

figure the receiver bias is determined as 2.78 ns, which is close to the value determined from GEONET, 2.29 ns. The difference between biases from the two methods is only

0.49 ns.

4.2 Accuracy of the simple method

The same procedure was applied to all the GEONET receivers and the receiver biases derived from the two methods are compared. A scatter plot of the GEONET-derived bias versus the fitted bias on June 17, 2001 is shown in Fig.11 for all receivers. The agreement between the GEONET b_r and the fitted one is amazingly good. Fig.12 gives the distribution of the difference between the

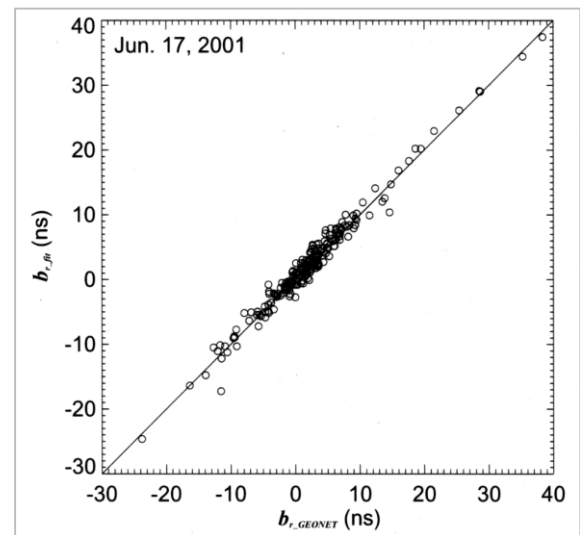


Fig. 11 Singly fitted bias is plotted versus GEONET derived bias for all receivers on Jun. 17, 2001.

The relationship $b_{r,GEONET} = b_{r,fit}$ is also shown for comparison.

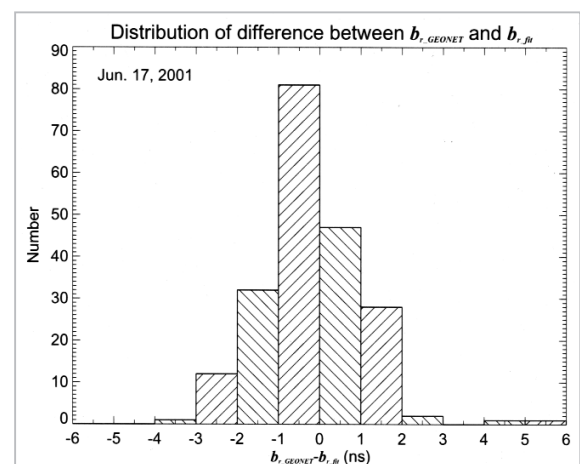


Fig. 12 Distribution of the number with the difference between GEONET derived bias and fitted bias for all receivers on Jun. 17, 2001.

GEONET and the fitted biases, $\Delta b_r (= b_{r_GEONET} - b_{r_fit})$ (hereafter, refer to as an error of fitted bias or simply an error) for the same data set. It can be seen that for most of the receivers (93%), the errors are within ± 2 ns.

Table 2 summarizes the percentage of the number of receivers for which the errors are within ± 2 ns for the 9 days analyzed. It is noticeable that on September 22, 2001 (265) the fitted bias has a large error for about 1/3 of the receivers. Specifically, these receivers are located at latitudes lower than 35°N as shown

in Fig.13, where the error's latitude dependence for the other days are also displayed. This is agreed with the large χ_g on the day 265 discussed in section 3.3. On the whole, the value of b_{r_fit} tends to be larger than that of b_{r_GEONET} for the receivers at lower latitudes ($< 30^\circ\text{N}$), and the error tends to increase with the decrease of latitude. This suggests that the ionospheric condition affect the bias determination by fitting for a single receiver. For further investigation of the error source, and hence the limit in the application of the

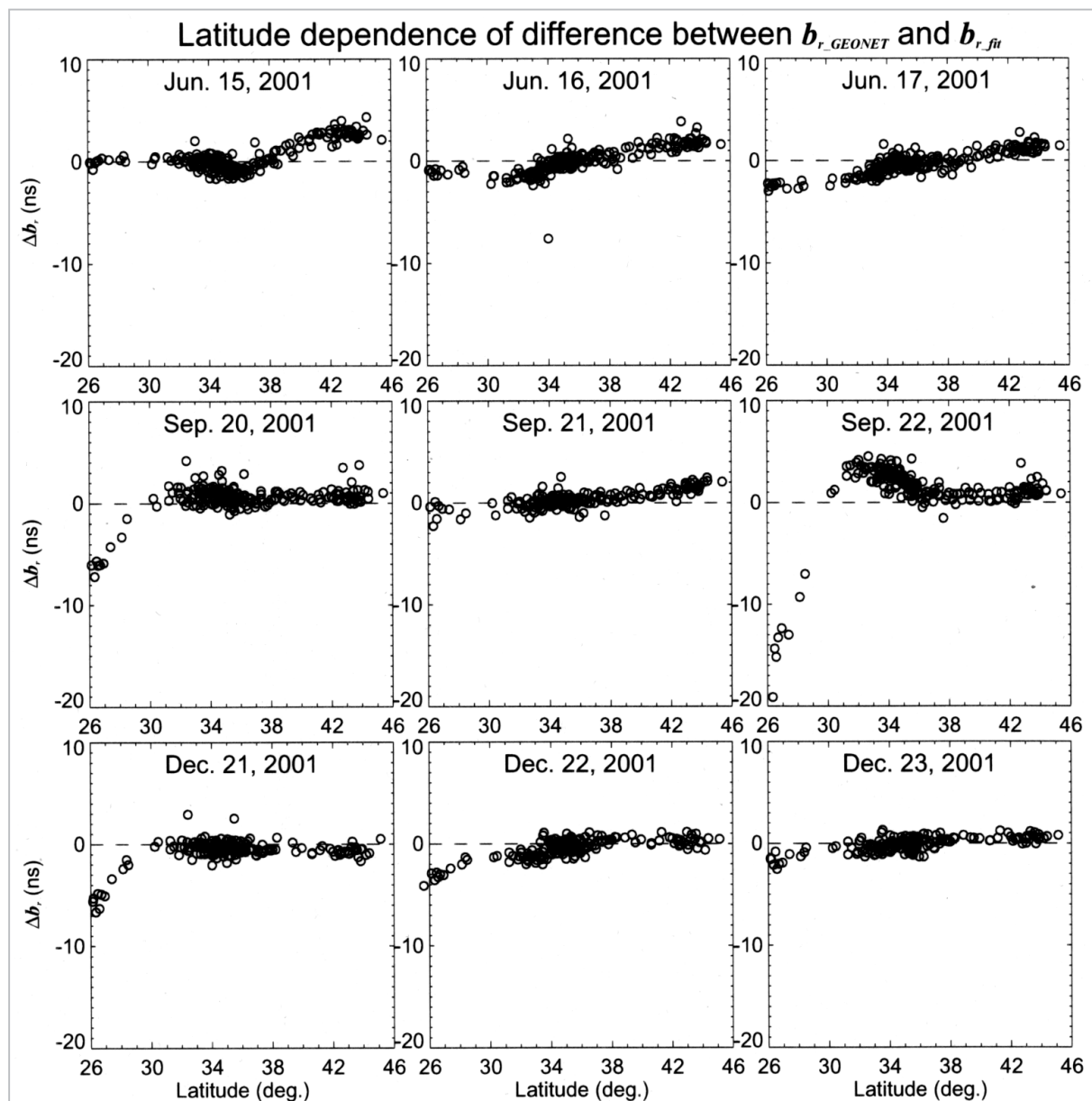


Fig. 13 Latitude dependence of the difference between biases determined from the two different methods for the 9 days analyzed. The dashed line referring to no difference is plotted in each panel for easy comparison.

Table 2 The percentage of the difference within ± 2 ns between GEONET derived receiver bias and single receiver fitted bias. The numbers in the first row refers to the day of year 2001.

DOY	166	167	168	263	264	265	355	356	357
Perc.	79%	91%	93%	90%	95%	69%	93%	94%	98%

method, the total standard deviation of the TECs to their mean, $\Sigma\sigma$, for each receiver was calculated by using the fitted receiver bias. The latitude variations of $\Sigma\sigma$ are shown in Fig.14. By comparing Figs.13 and 14, it can be noticed that a large value of $\Sigma\sigma$, or ill convergence, does not necessarily yield a large

error. Taking September 22, 2001 as an example, the error decreased with the increase of $\Sigma\sigma$ at latitudes lower than 30°N .

The latitude dependence of the $\Sigma\sigma$ and hence the bias error can be explained in terms of TEC latitude gradient and the equatorial anomaly, which are clearly depicted in Fig.14. Having high activity in the equinox, the equatorial anomaly is characterized by two electron density peaks (known as crest) in the vicinity of geomagnetic latitude of 15° symmetric to the geomagnetic equator, which corresponds to about 25°N geographically at Japan's longitude. For a receiver located at or

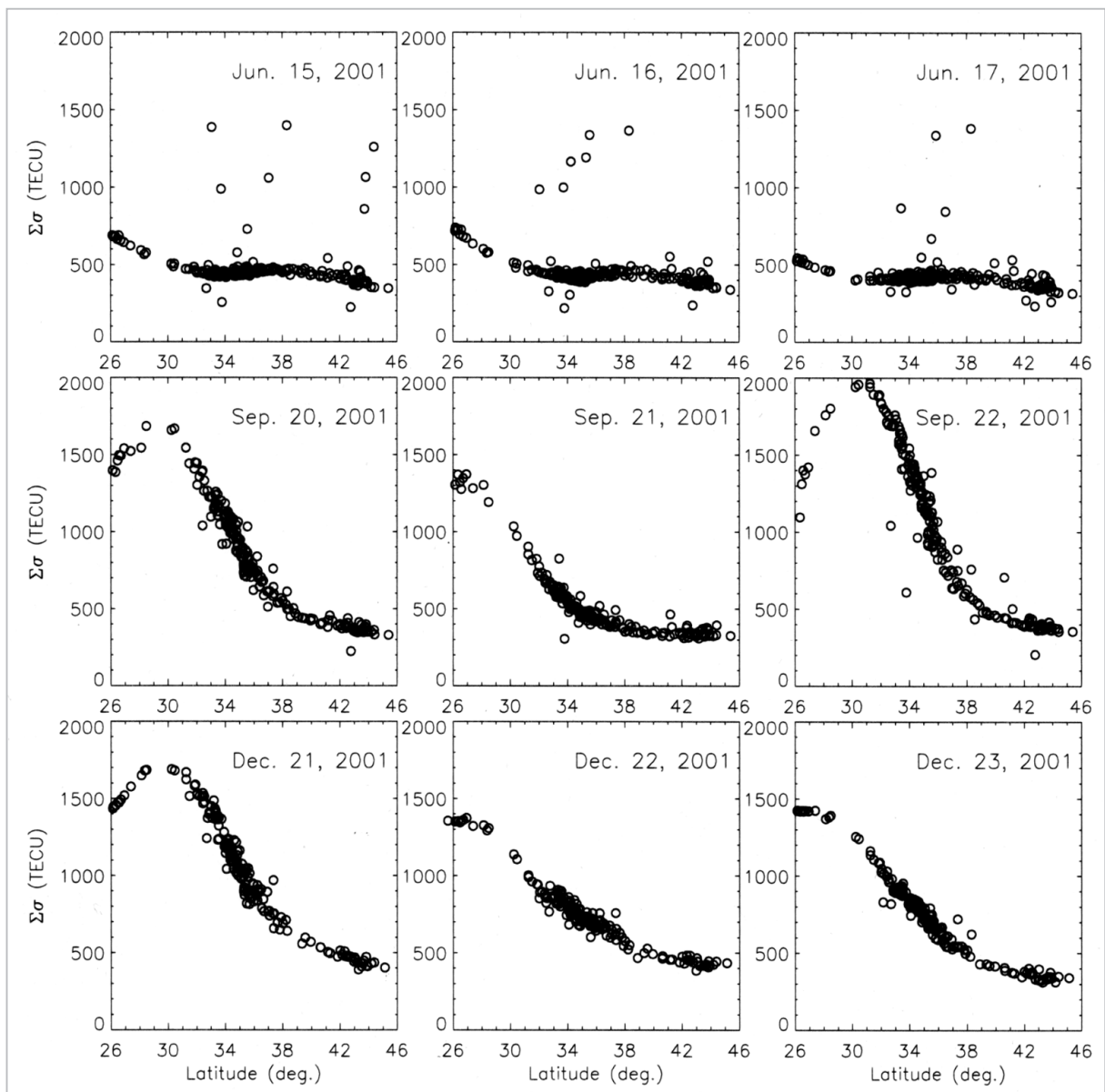


Fig.14 The variation of $\Sigma\sigma$ with latitude for the 9 days analyzed.

near the crest of equatorial anomaly, the satellites within the range tend to be distributed apart from the crest. The vertically converted *TECs* would have a mean smaller than the *TEC* through the crest. And the deviation of *TECs* from their mean, $\Sigma\sigma$, would be smaller than that of *TECs* with large latitude gradient or variance.

5 Summary

The dual GPS data from 209 GEONET receivers in Japan was used to determine *TEC* over Japan, as well as the biases of satellites and receivers. The paper also proposed a faster and simpler way to estimate a single receiver's bias as long as the satellite biases are known. The methods described herein have been applied to geomagnetically quiet days in the summer, the autumn and the winter.

The main results obtained in the biases estimation can be summarized as follows:

- (1) The standard deviation from the mean is from 0.076 ns to 0.664 ns for the 28 GPS satellite biases for 9 days over the six-month time span.
- (2) There are 93% of the receiver biases whose standard deviation is smaller than 2 ns from the mean for the 9 days. It can be as large as 4 ns for a few receivers.
- (3) The fitted bias for a single receiver is generally within ± 2 ns from GEONET derived bias. Larger deviation from GEONET derived bias tends to occur to those receivers at lower ($<35^\circ\text{N}$) in the autumn and winter. This is resulted from the steep latitude gradient in the local ionosphere probably with the development of the equatorial anomaly effects.

Concerning the GPS-derived *TEC*, the following has been found from a comparison with foF_2 :

- (1) The diurnal and seasonal variations in *TEC* and foF_2 show a high degree of conformity.

- (2) The ratio of *TEC* to the square of foF_2 also showed diurnal and seasonal variation. The daytime peak value in the winter was about twice that in the summer and autumn.

6 Conclusions

It can be concluded based on the results of an analysis of data obtained from GEONET that, the method described herein is efficient and qualified for use to derive the absolute *TEC*, and to determine the biases of GPS satellites and receivers. Since the day-to-day variation is small in satellite and receiver biases, it is only necessary that the instrumental biases be estimated or calibrated from time to time. This is especially true for satellite biases.

The proposed method for estimating a single receiver's bias is faster and sufficiently accurate for a receiver at mid-latitude. It has the potential to meet the requirement of being able to monitor the ionosphere in nearly real-time. It can be also applied to the receiver far from a GPS network. But the accuracy of fitting bias can be low for a receiver at lower latitude due to the effects of equatorial anomaly. This disadvantage can be avoided by determining the receiver bias at mid-latitude before its establishment at lower latitude.

The GPS-derived *TEC* is mainly contributed from the electrons in F2 region. It is shown from the ratio of *TEC* to the square of foF_2 that plasmaspheric electron content is larger in the winter than that in the summer or autumn.

Acknowledgments

We would like to thank the Geographical Survey Institute of Japan for convenient and free use of their GEONET GPS data. Thanks are also due to A. Saito, K. Hocke and Y. Otsuka for helpful discussions.

References

- 1 Blewitt, G., "An automatic editing algorithm for GPS data", *Geophys. Res. Lett.*, 17, 199-202, 1990.
- 2 Bevington, P. R., "Data reduction and error analysis for the physical sciences", McGraw- Hill, New York, 1969.
- 3 Coco, D. S., C. Coker, S. R. Dahlke, and J. R. Clync, "Variability of GPS satellite differential group delay biases", *IEEE Trans. Aerosp. Electron. Sys.*, 27, 931-938, 1991.
- 4 Ho, C. M., A. J. Mannucci, L. Sparks, X. Pi, U. J. Lindqwister, B. D. Wilson, B. A. Iijima, and M. J. Reys, "Ionospheric total electron content perturbations monitored by the GPS global network during two northern hemisphere winter storms", *J. Geophys. Res.*, 103, 26409-26420, 1998.
- 5 Hovath, I. and E. A. Essex, "Using observations from the GPS and TOPEX satellites to investigate night-time TEC enhancements at mid-latitudes in the southern hemisphere during a low sunspot number period", *J. Atmos. Sol. Terr. Phys.*, 62, 371-391, 2000.
- 6 Lanyi, G. E. and T. Roth, "A comparison of mapped and measured total ionospheric electron content using Global Positioning System and beacon satellites observations", *Radio Sci.*, 23, 483-492, 1988.
- 7 Lunt, N., L. Kersley, and G.J. Bailey, "The influence of the protonosphere on GPS Observations: Model simulations", *Radio Sci.*, 34, No. 3, 725-732, 1999.
- 8 Mannucci, A.J., B.D. Wilson, D.N. Yuan, C.H. Ho, U.J. Lindqwister, and T.F. Runge, A global mapping technique for GPS-derived ionospheric electron content measurements, *Radio Sci.*, 33, 565-582, 1998.
- 9 Miyazaki, S., T. Saito, M. Sasaki, Y. Hatanaka, and Y. Iimura, Expansion of GSI's nationwide GPS array, *Bull. Geogr. Surv. Inst.*, 43, 23-34, 1997.
- 10 Otsuka, Y., T. Ogawa, A. Saito, T. Tsugawa, S. Fukao, and S. Miyazaki, "A new technique for mapping of total electron content using GPS network in Japan", *Earth Planets Space*, 111-120, 2001.
- 11 Press, W.H., S. A. Teukolsky, W. T. Vetterling, and B. P. Flannery, "Numerical Recipes in Fortran 77", Cambridge University Press, 670-673, 1992.
- 12 Reiff, P. H., "The use and misuse of statistical analysis", in R. L. Carovillano and J. M. Forbes (Ed.), *Solar-Terrestrial Physics*, 493-522, 1983.
- 13 Sardón, E., A. Rius, and N. Zarraoa, "Estimation of the transmitter and receiver differential biases and the ionospheric total electron content from Global Positioning System observations", *Radio Sci.*, 29, 577-586, 1994.
- 14 Sardón, E. and N. Zarraoa, "Estimation of total electron content using GPS data: How stable are the differential satellite and receiver instrumental biases?", *Radio Sci.*, 32, 1899-1910, 1997.
- 15 Wilson, B. D., A. J. Mannucci, C. D. Edwards, and T. Roth, "Global ionospheric maps using a global network of GPS receivers", paper presented at the international Beacon Satellite Symposium, MIT, Cambridge, MA, July 6-12, 1992.
- 16 Wilson, B. D., A. J. Mannucci, and C. D. Edwards, "Subdaily northern hemisphere ionospheric maps using an extensive network of GPS receivers", *Radio Sci.*, 30, 639-648, 1995.



MA Guanyi, Dr. Sci

*Research Fellow, Ionosphere and Radio Propagation Group, Applied Research and Standards Division
Ionosphere*



MARUYAMA Takashi, Ph. D.

*Leader, Ionosphere and Radio Propagation Group, Applied Research and Standards Division
Upper Atmosphere Physics*

